Calculating the trap density of states in organic field-effect transistors from experiment: A comparison of different methods

Wolfgang L. Kalb* and Bertram Batlogg
Laboratory for Solid State Physics, ETH Zurich, 8093 Zurich, Switzerland
(Received 9 October 2009; published 19 January 2010)

The spectral density of localized states in the band gap of pentacene (trap DOS) was determined with a pentacene-based thin-film transistor from measurements of the temperature dependence and gate-voltage dependence of the contact-corrected field-effect conductivity. Several analytical methods to calculate the trap DOS from the measured data were used to clarify, if the different methods lead to comparable results. We also used computer simulations to further test the results from the analytical methods. Most methods predict a trap DOS close to the valence-band edge that can be very well approximated by a single exponential function with a slope in the range of 50–60 meV and a trap density at the valence-band edge of $\approx 2 \times 10^{21}$ eV^{-1} cm^{-3}. Interestingly, the trap DOS is always slightly steeper than exponential. An important finding is that the choice of the method to calculate the trap DOS from the measured data can have a considerable effect on the final result. We identify two specific simplifying assumptions that lead to significant errors in the trap DOS. The temperature dependence of the band mobility should generally not be neglected. Moreover, the assumption of a constant effective accumulation-layer thickness leads to a significant underestimation of the slope of the trap DOS.

DOI: 10.1103/PhysRevB.81.035327 PACS number(s): 73.61.Ph, 73.20.At, 73.20.Hb, 85.30.De

I. INTRODUCTION

World-wide research on organic field-effect transistors is at a high level as this new technology is poised to enter the market.[1,2] An appealing feature of this technology is that organic semiconductors can be deposited by thermal evaporation or from solution at low cost on large areas while keeping the substrates close to room temperature. Consequently, organic semiconductors are promising candidates for future flexible and low-cost electronics.

The mobility of charge carriers in organic field-effect transistors is comparable to the mobility in hydrogenated amorphous silicon thin-film transistors (1 cm^2/Vs) and thus is already adequate for many applications.[3–6] In addition to a high mobility, useful organic transistors must have a near zero threshold voltage, a steep subthreshold swing and a high electrical and environmental stability. The transistor parameters and stability of organic field-effect transistors are intimately related to the efficiency of the charge-transport mechanism and the extend of charge-carrier trapping in extrinsic traps. The main scientific challenge thus is to clarify the nature of the charge-transport mechanism and the microscopic origin of charge-carrier traps in organic field-effect transistors.

Field-effect transistors can be used to determine the underlying spectral density of localized states in the band gap, i.e., the trap densities as a function of energy (trap DOS). This has been extensively done with thin-film transistors (TFT's) employing amorphous semiconductors or with TFT's based on polycrystalline silicon.[7–19] This approach is expected to be of great value for the understanding of any novel semiconductor in a field-effect transistor including organic small-molecule semiconductors, polymeric semiconductors, or ZnO.[20]

The research efforts to calculate the trap DOS from measurements of organic field-effect transistors have increased only recently. On the one hand, the density-of-states function can be calculated from the linear-regime-transfer characteristics in a straightforward fashion with an analytical method.[21–27,29–35,59] This approach has the advantage of giving an unambiguous result but errors may result from the various simplifying assumptions. On the other hand, a density-of-states function can be postulated *a priori* and the corresponding transistor characteristics can be calculated by means of a suitable computer program. The density-of-states function is then iteratively refined until good agreement between the measured characteristic and the computer-simulated curve is achieved.[36–42]

Several analytical methods have been used to calculate the trap DOS from transfer characteristics of organic field-effect transistors. In order to eventually clarify the microscopic origin of charge-carrier traps in organic field-effect transistors, it is highly desirable to quantitatively compare the results from various experiments and from various research groups. An important prerequisite to such a systematic comparison is to test if the different analytical methods lead to comparable results. We applied the most frequently used analytical methods to the same set of measured transfer characteristics. Moreover, we applied a computer simulation program to determine a trap DOS that leads to simulated transfer characteristics closely matching the measured data.

In the following we are dealing with pentacene and *p*-type conduction. For convenience the charge carriers are called holes although they may be of pronounced polaronic character.[43] Moreover, we use terms such as valence-band edge (VB), band mobility, or effective density of extended states. However in order to apply the calculation methods described below, we do not necessarily need to have band transport or the existence of extended states. The calculation methods may be applied as long as the charge transport can be described by a transport level with a distribution of trap states below this transport level (trap-controlled transport).[44]

 ©2010 The American Physical Society

We begin by summarizing the widely used analytical description of an organic field-effect transistor. This description is only valid for samples with a low trap density and negligible contact resistances. The trapping and release times are assumed to be much shorter than the time necessary to measure a transistor characteristic, i.e., we have no current hysteresis. In Sec. III we present the trap DOS calculated with the different methods for a pentacene TFT with a SiO_2 gate dielectric, i.e., a sample with a significantly high trap density. The essential equations of the different analytical methods are also given in this section along with specific details about the use of the calculation methods.

II. ANALYTICAL DESCRIPTION OF AN IDEAL FIELD-EFFECT TRANSISTOR

In the linear regime ($|V_d| \ll |V_g - V_t|$), the drain current I_d of an ideal field-effect transistor is given by

$$I_d = \frac{W}{L}\mu_0 C_i (V_g - V_t) V_d, \tag{1}$$

where C_i is the capacitance per unit area, W and L are the channel width and length, V_g and V_d are the gate voltage and the drain voltage, and μ_0 is the band mobility which is independent of gate voltage. Equation (1) predicts a linear dependence of the drain current on the effective gate voltage $I_d \propto (V_g - V_t)$. A linear regression of the measured transfer characteristic thus yields the band mobility μ_0 and the threshold voltage V_t. The threshold voltage is defined as the gate voltage above which essentially all of the incrementally added gate-induced charge is mobile (free). The threshold voltage depends on the trap density in the device and on the flatband voltage V_{FB}. The flatband voltage is the gate voltage which needs to be applied in order to enforce flat bands at the insulator-semiconductor interface. A nonzero flatband voltage can result from a difference of the Fermi level in the semiconductor and in the gate electrode. More importantly, the flatband voltage is influenced by charge that is permanently trapped at the insulator-semiconductor interface or within the gate dielectric.

The drain current in the saturation regime ($|V_d| \geq |V_g - V_t|$) quadratically depends on gate voltage, i.e.,

$$I_d = \frac{W}{L}\frac{\mu_0 C_i}{2}(V_g - V_t)^2. \tag{2}$$

Fitting a straight line to the square root of the measured drain current yields the band mobility μ_0 and the threshold voltage V_t. This ideal behavior can be observed in organic field-effect transistors with a low trap density. For example in Fig. 1 we show the near-ideal transfer characteristic of a pentacene single-crystal field-effect transistor (SC-FET) with a Cytop™ fluoropolymer gate dielectric.[28]

The onset voltage V_{on} and the subthreshold swing S are other important device parameters. The onset voltage is defined as the gate voltage where the drain current exceeds the noise level which typically is at 10^{-12} A (see Fig. 2). The subthreshold swing is a measure of how easily a transistor can be switched from the off-state to the on-state. It is defined as[45]

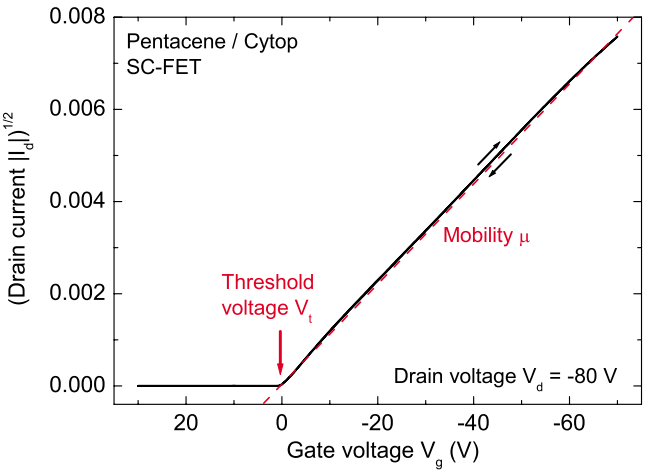

FIG. 1. (Color online) High-performance pentacene single-crystal field-effect transistor (SC-FET) with a Cytop™ fluoropolymer gate dielectric. The graph shows the square root of the drain current (full black line) and the dashed red line (dashed gray line in print) is a linear fit of the measured data. The square root of the drain current linearly depends on gate voltage in accordance with the well-known field-effect transistor equation for the saturation regime. This linear dependence is a mark of the low trap density at the insulator-semiconductor interface as well as the high field-effect mobility of $\mu = 1.4$ cm^2/Vs and the near-zero threshold voltage.

$$S = \frac{dV_g}{d(\log I_d)}. \tag{3}$$

With the simplistic assumption that both the density of deep bulk traps N_{bulk} and the density of (deep) interface traps N_{int} are independent of energy, the subthreshold swing may be written as[46]

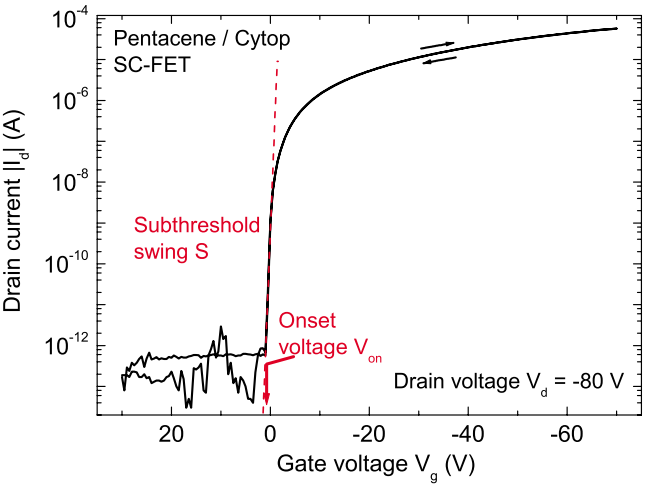

FIG. 2. (Color online) Same data as in Fig. 1 of a pentacene/Cytop SC-FET plotted on a logarithmic scale. The forward and reverse sweeps are shown. The very low trap density in the active region of the transistor manifests itself in several desirable properties: near-zero onset voltage V_{on}, very steep subthreshold swing of $S = 0.3$ V/dec, as estimated from the dashed red (gray) line, and negligible current hysteresis.

$$S = \frac{kT \ln 10}{e}\left[1 + \frac{e}{C_i}(\sqrt{\epsilon_s N_{bulk}} + eN_{int})\right]. \quad (4)$$

This may be simplified as follows:

$$S = \frac{kT \ln 10}{e}\left[1 + \frac{e^2}{C_i}N_{\square}\right]. \quad (5)$$

Both the deep bulk traps and the interface traps contribute to the trap density $N_{\square}$ (per unit area and unit energy).[47,48] The subthreshold swing thus is a simple measure of the deep trap density. Figure 2 shows the same data as in Fig. 1 on a logarithmic scale. The subthreshold swing is as steep as $S = 0.3$ V/dec. With Eq. (5) and $C_i = 4.3$ nF/cm^2 we calculate a trap density from S as low as $N_{\square} = 1.1 \times 10^{11}$ cm^{-2} eV^{-1}. Assuming an effective accumulation-layer thickness of $a = 7.5$ nm this results in a volume trap density of $N = N_{\square}/a = 1.5 \times 10^{17}$ cm^{-3} eV^{-1}.

If the experimental transfer characteristics are linear in the linear regime and quadratic in the saturation regime, the approach described above is self-consistent and the extracted mobility μ_0 and threshold voltage V_t have a clear meaning, i.e., μ_0 is the band mobility and V_t is the voltage above which the incrementally added gate-induced charge is placed in the valence band. In samples with an increased trap density, the drain current in the linear regime may however increase faster than linearly. For example, this can be seen in the lower panel of Fig. 3 where we show the measured transfer characteristics of a pentacene TFT with SiO_2 gate dielectric for several temperatures. The transconductance $(\partial I_d/\partial V_g)_{V_d}$ now increases monotonically with gate voltage. The percentage of the gate-induced holes that are free increases with gate voltage and this leads to the "superlinear" transfer characteristics. Strictly speaking, the threshold voltage is not reached even at relatively large gate voltages. Equations (1) and (2) are not suitable for this type of transistor.[49,50] This is similar to the case of amorphous silicon field-effect transistors, where the trap densities are substantial.[51] We note that for this TFT, the gate capacitance is $C_i = 13.3$ nF/cm^2. This is about three times larger than the capacitance for the SC-FET in Figs. 1 and 2. The difference between the two types of transistors is even more drastic than it appears when comparing the graphs.

III. QUANTIFICATION OF THE TRAP DOS

Field-effect transistors can be used to quantify the underlying trap DOS if a more sophisticated description of the device physics is used. We applied several analytical methods to the linear-regime-transfer characteristics in Fig. 3. We also applied a simulation program to determine a trap DOS that leads to simulated transfer characteristics closely matching these measured transfer characteristics. Moreover, the results were compared to the crude estimate of the trap density from the subthreshold swing [Eq. (5)]. We used a dielectric constant of $\epsilon_i = 3.9$ for SiO_2 and $\epsilon_s = 3.0$ for pentacene.[52,53] The thickness of the SiO_2 gate dielectric was $l = 260$ nm and the pentacene film was $d = 50$ nm thick. The channel was $L = 450$ μm long and $W = 1000$ μm wide.

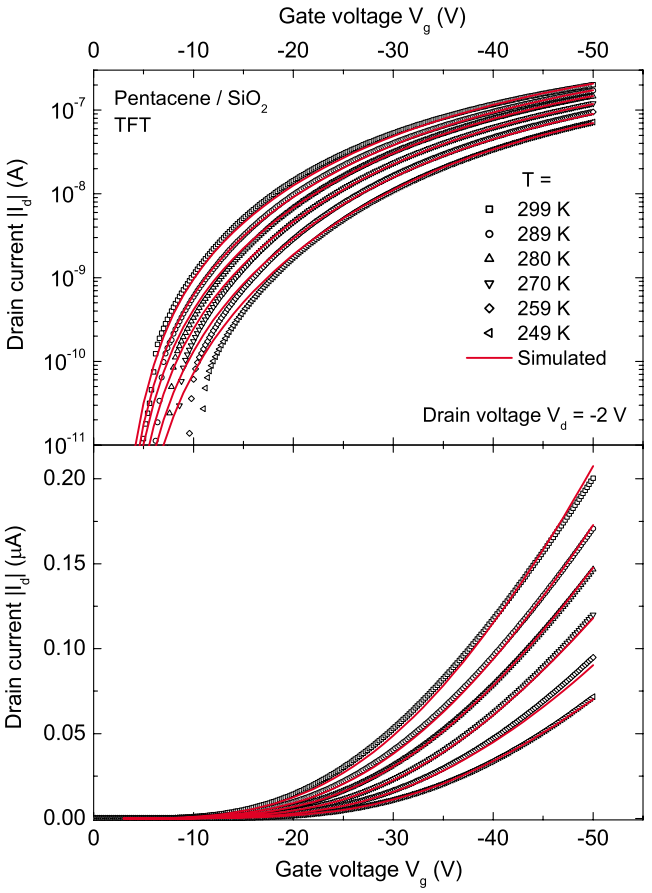

FIG. 3. (Color online) Transfer characteristics of a pentacene-based thin-film transistor (TFT) with a SiO_2 gate dielectric measured at various temperatures (symbols). The upper and lower panels show the same data on a logarithmic and linear scale. The red lines (gray in print) are computer-simulated transfer characteristics. The increased subthreshold swing (upper panel) and the reduced field-effect mobility ($\mu \approx 0.2$ cm^2/Vs at $V_g = -50$ V and $T = 299$ K) are a result of a relatively high trap density. The high trap density also results in the drain current to increase faster than linearly in the linear regime (lower panel).

All analytical methods and the simulation program are based on the following simplifying assumptions: (i) The organic semiconductor is homogenous perpendicular to the insulator-semiconductor interface. (ii) Insulator surface states only introduce an initial band bending without applied field, i.e., contribute to a nonzero flatband voltage V_{FB}. As a consequence of these assumptions we obtain an effective trap DOS. In the case of TFT's with polycrystalline films, the trap densities to be determined are an average over intragrain and intergrain regions and may also be influenced, to some extend, by trap states on the surface of the gate dielectric.

A. Analytical methods

Several additional assumptions are made to simplify the analytical methods: (i) The charge density is homogenous along the transistor channel (from source to drain). (ii) For the trapped holes, the Fermi function is approximated by a step function (zero-temperature approximation). (iii) The va-

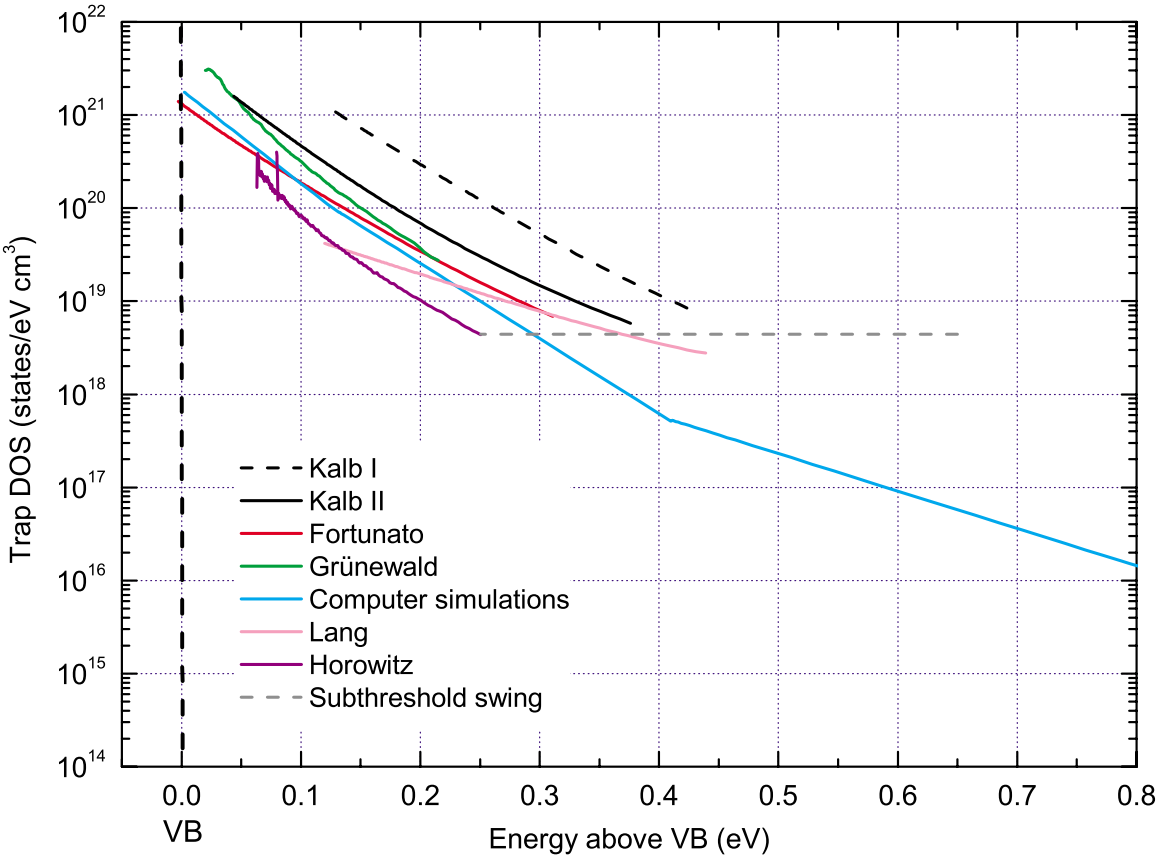

FIG. 4. (Color online) Spectral density of localized states in the band gap of pentacene (trap DOS) as calculated with several methods from the same set of measured data. The energy is relative to the valence-band edge (VB). The estimate from the subthreshold swing (dashed gray line) assumes the trap DOS not to depend on energy and can only be regarded as a rough estimate for the traps slightly above the Fermi energy. All other methods result in a trap DOS that increases slightly faster than exponentially with energy. The choice of the method to calculate the trap DOS has a considerable effect on the final result.

lence band is approximated as a discrete energy level at the valence-band edge E_V with an effective density of extended states N_V. The occupation of these extended states is calculated with the Boltzmann function. (iv) The temperature dependence of the Fermi energy E_F as well as of the interface potential V_0 is neglected (neglect of the statistical shift).

The first assumption is appropriate only if the transfer characteristics are measured at a low drain voltage. In that case we can assume the "unperturbed" situation where charge is accumulated by a gate voltage in a metal-insulator-semiconductor structure but no drain voltage is applied.[50]

The final results from the different methods are summarized in Fig. 4 and Table I along with the result from the simulation program. The parameters N_0 and E_0 in Table I were obtained by fitting to each trap DOS an exponential function

$$N(E) = N_0 \exp(-E/E_0). \tag{6}$$

Figure 4 and Table I also contain the trap density as estimated from the subthreshold swing of $S=2.4$ V/dec with Eq. (5) and an effective accumulation layer thickness of $a=7.5$ nm. Some methods also lead to an estimate of the band mobility μ_0 (see Table I).

TABLE I. Parameters resulting from different methods to calculate the trap DOS and the trap DOS from each method is shown in Fig. 4. The different methods were applied to the same set of measured data (Fig. 3). To obtain the parameters N_0 and E_0, an exponential function $N(E)=N_0 \exp(-E/E_0)$ was fitted to the calculated trap DOS in each case. Most methods lead to a slope in the range of $E_0=50-60$ meV and to a trap density at the valence-band edge of $N_0 \approx 2\times10^{21}$ eV^{-1} cm^{-3}. Some methods also lead to an estimate of the band mobility μ_0.

Method	Reference	N_0 (eV^{-1} cm^{-3})	E_0 (meV)	μ_0 [a] (cm^2/Vs)
Kalb I	32	8.5×10^{21}	60	0.7
Kalb II	This paper	2.4×10^{21}	59	
Fortunato	18 and 26	1.1×10^{21}	60	
Grünewald	8 and 10	4.0×10^{21}	41	
Computer sim.	40	1.5×10^{21}	50	0.3
Lang[b]	25	1.1×10^{20}	115	17
Horowitz	21	7.0×10^{20}	48	0.2
Subthreshold swing[b,c]	46–48	$N=4.4\times10^{18}$		

[a]Band mobility at $T=299$ K.
[b]Effective accumulation-layer thickness of $a=7.5$ nm.
[c]Assumption: trap DOS independent of energy.

The final results in Fig. 4 and Table I are discussed in Sec. IV. The simulations are described in more detail in Sec. III B. In the following we describe the different analytical methods and give some specific details about how the methods were used.

All methods require linear-regime-transfer characteristics measured at several temperatures (as in Fig. 3). The exception is the method by Grünewald *et al.* which only requires a single linear-regime-transfer characteristic measured at one temperature (e.g., room temperature). In order to calculate the trap DOS from the transfer characteristics $I_d(V_g)$ we need the field-effect conductivity σ and the field-effect mobility μ at first. Provided that contact effects are negligible, the drain current in the linear regime may be written as

$$I_d = \frac{W}{L}\sigma V_d \tag{7}$$

and the field-effect conductivity σ is

$$\sigma = \mu C_i (V_g - V_{FB}). \tag{8}$$

V_{FB} is the flatband voltage and μ is the (gate-voltage dependent) field-effect mobility, i.e., an effective mobility in contrast to the band mobility μ_0. The field-effect conductivity can be calculated from

$$\sigma(V_g) = \frac{L}{W}\frac{I_d}{V_d}. \tag{9}$$

The calculation of the field-effect mobility from measurements of organic field-effect transistors is still controversial for samples with an increased trap density.[50] If we differentiate Eq. (7) with respect to gate voltage, we have[54]

$$\frac{\partial I_d}{\partial V_g} = \frac{W}{L}C_i V_d \left[\mu + (V_g - V_{FB})\frac{\partial \mu}{\partial V_g} \right]. \tag{10}$$

The field-effect mobility is most often calculated from

$$\mu(V_g) = \frac{L}{W V_d C_i}\left(\frac{\partial I_d}{\partial V_g}\right)_{V_d}, \tag{11}$$

which means that the second term in Eq. (10) is generally neglected.

Contact effects can introduce significant errors when the field-effect conductivity and the field-effect mobility are calculated.[55,56] The contact-corrected field-effect conductivity can be calculated from gated four-terminal measurements according to

$$\sigma(V_g) = \frac{L'}{W}\frac{I_d}{V_d'}. \tag{12}$$

L' is the distance between the voltage-sensing electrodes and $V_d' = V_1 - V_2$ is the voltage drop between these electrodes.[32,59] The effective field-effect mobility μ is not influenced by parasitic contact resistances when calculated from gated four-terminal measurements according to

$$\mu(V_g) = \frac{L'}{W V_d' C_i}\left(\frac{\partial I_d}{\partial V_g}\right)_{V_d}. \tag{13}$$

The mobilities as calculated with Eq. (11) or Eq. (13) overestimate the true field-effect mobilities to some extend.[54] This is because for trap-controlled transport, the mobility increases with gate voltage. This leads to a positive second term in Eq. (10) which is neglected in Eq. (11) [and Eq. (13)]. However, the use of Eq. (11) [or Eq. (13)] is advantageous because the definition and extraction of a flatband voltage V_{FB} is circumvented. Moreover, this approach to the field-effect mobility is most often used which guarantees a good comparability of the mobility values. Consequently, we choose Eq. (13) [the contact-corrected version of Eq. (11)] to calculate the field-effect mobility in the present study. Alternatively, the contact-corrected field-effect mobility could also be calculated from[54]

$$\mu = \frac{L'}{W V_d' C_i}\frac{I_d}{(V_g - V_{FB})}. \tag{14}$$

In that case we would not need to differentiate the measured data but a reliable estimate of the flatband voltage (threshold voltage) would be required.[54]

In Fig. 3 we show the measured transfer characteristics $I_d(V_g)$ from gated four-terminal measurements. In addition to the drain current $I_d(V_g)$, the potentials $V_1(V_g)$ and $V_2(V_g)$ between the grounded source electrode and the respective voltage-sensing electrode were measured simultaneously while keeping the source-drain voltage constant. This was done by connecting the source of the transistor to the ground connector of an HP 4155A parameter analyzer and by measuring the channel potentials V_1 and V_2 with two additional source/monitor units (SMU's) in the "source current—measure voltage" mode with a sourced current of 0 A. For all analytical methods we used the four-terminal conductivity $\sigma = \sigma(V_g)$ as derived from gated four-terminal measurements with Eq. (12) and the field-effect mobility was calculated according to Eq. (13). This allowed for the calculation of a trap DOS that is free from contact artifacts.[32,59] Moreover, we only used currents above $|I_d| = 1$ nA for the calculation of trap DOS (1 nA limit).[32] For the following description of the analytical methods, Figs. 2 and 3 in Ref. 32 are useful.

1. Method by Lang et al.

For this method (Ref. 25), the activation energy $E_a(V_g)$ is defined by

$$\sigma(V_g) = A \exp\left(-\frac{E_a}{kT}\right) \tag{15}$$

and A is assumed to be a constant. The activation energy is determined from the measured data with a linear regression of $\ln\sigma$ vs $1/T$ for each gate voltage according to $\ln\sigma = \ln A - E_a/kT$. The energetic difference between the Fermi level E_F of the sample and the valence-band edge at the insulator-semiconductor interface is approximated with the measured activation energy $E_a(V_g)$ of the field-effect conductivity σ, i.e.,

$$E_a \approx E_V - E_F - eV_0. \tag{16}$$

$V_0 = |V(x=0)|$ is the potential right at the insulator-semiconductor interface. The x direction is normal to this

interface. E_V is the energy of the valence-band edge far from the insulator-semiconductor interface (at $x=d$, Fig. 3 in Ref. 32). The underlying idea is the following: a change in the gate voltage by ΔV_g leads to a shift of the activation energy E_a (i.e., of the effective Fermi level $\tilde{E}_F=E_F+eV_0$ at the insulator-semiconductor interface) by $\Delta\tilde{E}_F \approx \Delta E_a$. The change in gate voltage ΔV_g corresponds to a total hole density per unit area of $\Delta P=C_i\Delta V_g/e$. Then, the abrupt approximation is made: the charge in the accumulation layer is constant up to a distance a from the insulator-semiconductor interface and zero for larger distances. For the present method, it is assumed that the parameter a does not depend on gate voltage.[25] Consequently, we have a change in the volume hole density of $\Delta p=\Delta P/a$ close to the insulator-semiconductor interface. By neglecting the free charge we can estimate the trap density to be

$$N = \Delta p/\Delta E_a = \frac{C_i}{ea}\left(\frac{\Delta E_a}{\Delta V_g}\right)^{-1}. \tag{17}$$

If one replaces the difference quotient in Eq. (17) by the respective derivative we have the final result

$$N(E) = \frac{C_i}{ea}\left(\frac{dE_a}{dV_g}\right)^{-1}. \tag{18}$$

Consequently, the function $N(E)$ is calculated with Eq. (18) and $N(E)$ is plotted as a function of the energy $E=E_a(V_g) \approx E_V-E_F-eV_0$.[25]

The band mobility μ_0 may be estimated with

$$\mu_0 = \mu \exp\left(\frac{E_a}{kT}\right) \tag{19}$$

by introducing the value of the measured activation energy E_a and the field-effect mobility μ at a fixed and sufficiently high gate voltage V_g.[57]

We now give some specific details about the application of this method to our data. The activation energy $E_a=E_a(V_g)$ was determined according to Eq. (15) and is shown in Fig. 5. The activation energy $E_a(V_g)$ was then represented by a smooth fit (red line in Fig. 5, gray line in print) in order to suppress the noise in the data. We used an effective accumulation-layer thickness of $a=7.5$ nm.[25] The band mobility μ_0 was calculated with Eq. (19) for a high gate voltage of $V_g=-50$ V and $T=299$ K.

2. Method by Horowitz et al.

Also for this method (Ref. 21) the abrupt approximation is made. However, in contrast to the method by Lang *et al.*, the present method allows for a gate-voltage dependence of the effective accumulation-layer thickness $a=a(V_g)$. As a consequence of the abrupt approximation, the potential $V(x)$ in the organic semiconductor is given by

$$V(x) = V_0\left(1-\frac{x}{a}\right)^2 \tag{20}$$

with the interface potential

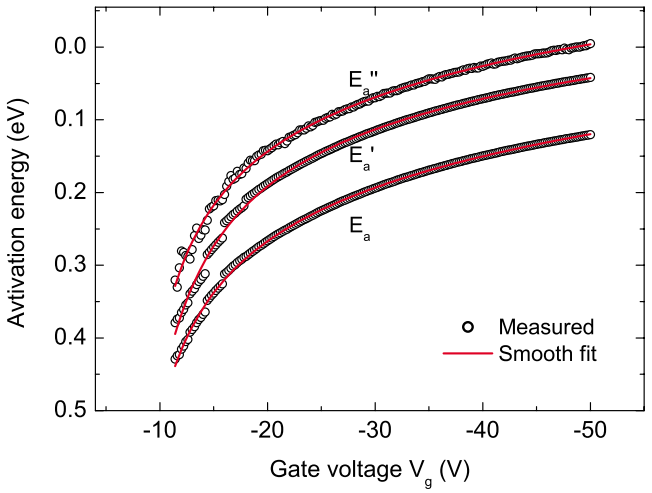

FIG. 5. (Color online) Activation energies E_a, E_a', and E_a'' as determined with linear regressions according to Eqs. (15), (43), and (30). The graph also shows a smooth fit of the activation energies in each case (red lines, gray in print). There is a significant difference between E_a, E_a', and E_a''.

$$V_0 \approx a\frac{C_iU_g}{2\epsilon_0\epsilon_s}. \tag{21}$$

$U_g=|V_g-V_{FB}|$ is the gate voltage above the flatband voltage V_{FB}. With the total hole density per unit area $P=C_iU_g$ and Eq. (21) we obtain an equation for the total volume hole density p which is

$$p = \frac{P}{a} \approx \frac{C_i^2U_g^2}{2\epsilon_0\epsilon_s eV_0}. \tag{22}$$

Assuming again the abrupt approximation, it can be shown that

$$eV_0 = E_V - E_F - kT\ln\left(\frac{\mu_0 N_V kT\epsilon_0\epsilon_s}{\mu C_i^2U_g^2}\right). \tag{23}$$

$\mu=\mu(V_g)$ is the gate-voltage-dependent field-effect mobility as calculated with Eq. (13). N_V is the effective density of extended states. For each temperature, the trap DOS is now calculated separately. To do so, a value of the product μ_0N_V is assumed *a priori* and the interface potential V_0 is calculated with Eq. (23). We note that this also requires an estimate of the difference between the Fermi energy and the energy of the valence-band edge far from the insulator-semiconductor interface E_V, i.e., an estimate of E_V-E_F. $V_0=V_0(V_g)$ from Eq. (23) is used to calculate the volume hole density p with Eq. (22). The Fermi function is approximated by a step function (zero-temperature approximation). Its derivative then is a delta function. Consequently, the trap DOS is eventually obtained by numerically differentiating the hole density p from Eq. (22) with respect to the interface potential V_0 from Eq. (23), i.e.,

$$N(E) \approx \frac{1}{e}\frac{dp(V_0)}{dV_0}. \tag{24}$$

The trap densities from Eq. (24) are finally plotted as a function of the energy $E=E_V-E_F-eV_0$ as calculated with Eq. (23). The trap DOS from the measurements at different temperatures will generally not coincide at first. The procedure is thus repeated for different values of the product $\mu_0 N_V$ until the trap DOS curves calculated from the data taken at different temperatures, coincide.

The band mobility μ_0 is calculated from the final parameter $\mu_0 N_V$ by assuming a value of the effective density of extended states N_V. If N_V is fixed, μ_0 is the adjustable parameter.

We proceed by giving specific details about the use of this method. We estimated that $E_V-E_F=0.5$ eV. In order to determine $U_g=|V_g-V_{FB}|$, the flatband voltage V_{FB} was taken to be equal to the device onset voltage at room temperature. We thus have $V_{FB}=-4.6$ V. Moreover, the effective density of extended states N_V was assumed to be equal to the density of the pentacene molecules, i.e., $N_V=3\times10^{21}$ cm^{-3}. For example, the trap densities were calculated from the measurements at different temperatures with $\mu_0=2$ cm^2/Vs and the result is shown in the upper panel of Fig. 6. The trap densities from the different temperatures do not coincide. The procedure was repeated for different values of μ_0. For $\mu_0=0.2$ cm^2/Vs the energetic distributions of traps do coincide (lower panel of Fig. 6). This trap DOS was taken as the final result along with the band mobility of $\mu_0=0.2$ cm^2/Vs.

3. Method by Fortunato et al.

This method (also called temperature method) is described in Refs. 18 and 19. The trap DOS is calculated with

$$N(E) = \frac{\epsilon_0\epsilon_s}{2e}\frac{\partial^2}{\partial V_0^2}\left(\left.\frac{dV(x)}{dx}\right|_{x=0}\right)^2. \tag{25}$$

The electric field dV/dx in Eq. (25) may be written as

$$\left.\frac{dV(x)}{dx}\right|_{x=0} = \frac{\epsilon_i}{\epsilon_s}\frac{U_g-V_0}{l}. \tag{26}$$

The interface potential V_0 in Eqs. (25) and (26) is obtained as described in the following. First of all, the derivative of the field-effect conductivity can be written as

$$\frac{d\sigma}{dV_g} = \mu_0\frac{N_V\epsilon_0\epsilon_i}{lp(V_0)}\exp\left(-\frac{E_V-E_F-eV_0}{kT}\right) \tag{27}$$

and both the band mobility μ_0 and the exponential factor depend on temperature.[18] It can be shown that the total hole density $p(V_0)$ varies much less with temperature than the exponential term in Eq. (27).[18] As described in the following, the calculation of a normalized field-effect conductivity σ' eliminates the temperature dependence due to the band mobility μ_0 in Eq. (27).[19,26] The field-effect mobility at RT and at each reduced temperature T are calculated with Eq. (13). Then, the normalized field-effect conductivity σ' is calculated for each temperature according to

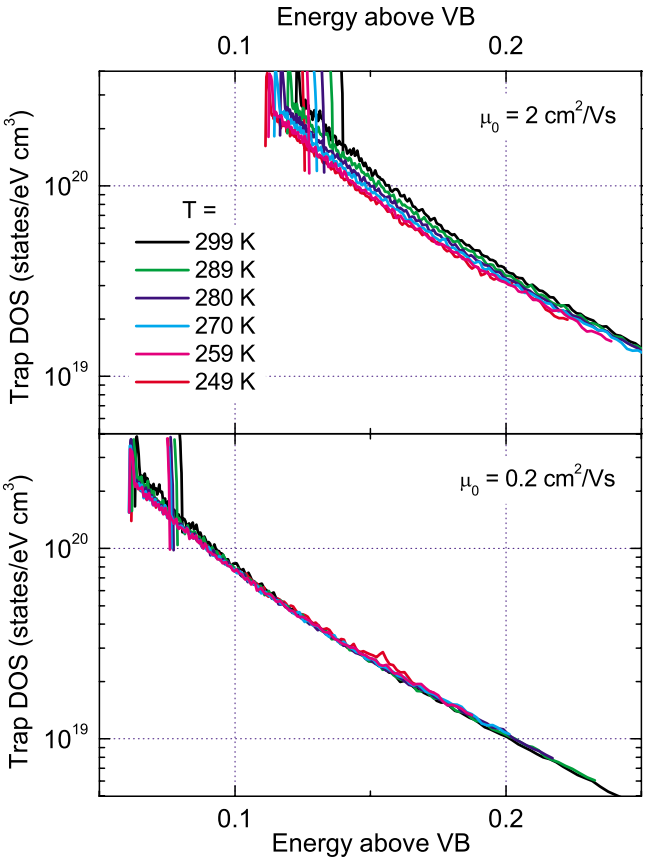

FIG. 6. (Color online) Trap densities calculated with the method by Horowitz *et al.* from the measurements at different temperatures. The band mobility μ_0 is an adjustable parameter in this method. Upper panel: $\mu_0=2$ cm^2/Vs and lower panel: $\mu_0=0.2$ cm^2/Vs. For $\mu_0=0.2$ cm^2/Vs the trap densities from the measurements at different temperatures coincide.

$$\sigma' = \sigma\frac{\mu^{\mathrm{RT}}}{\mu^T} \approx \sigma\frac{\mu_0^{\mathrm{RT}}}{\mu_0^T}. \tag{28}$$

μ^{RT} and μ^T in Eq. (28) are the field-effect mobilities at RT and at a reduced temperature T evaluated at a fixed and sufficiently high gate voltage. μ_0^{RT} and μ_0^T are the respective band mobilities.[19,26] Clearly, the derivative of the normalized field-effect conductivity may now be written as

$$\frac{d\sigma'}{dV_g} = \mu_0^{\mathrm{RT}}\frac{N_V\epsilon_0\epsilon_i}{lp(V_0)}\exp\left(-\frac{E_V-E_F-eV_0}{kT}\right) \tag{29}$$

and the exponential term is the only term with a temperature dependence [the temperature dependence of $p(V_0)$ is neglected]. Consequently, the activation energy E_a'' as determined with linear regressions according to

$$\frac{d\sigma'}{dV_g} \propto \exp\left(-\frac{E_a''}{kT}\right) \tag{30}$$

is approximately equal to the difference between the Fermi energy and the valence-band edge at the insulator-semiconductor interface, i.e.,

$$E_a'' \approx E_V - E_F - eV_0. \tag{31}$$

Once $E_a''(V_g)$ is known, the interface potential $V_0(V_g)$ can be calculated with Eq. (31) assuming *a priori* a value for the difference $E_V - E_F$. Then we can calculate the electric field with Eq. (26). The result is finally introduced in Eq. (25) and the numerical differentiation with respect to V_0 from Eq. (31) eventually yields the trap DOS as a function of energy $E = E_a'' \approx E_V - E_F - eV_0$.

It is instructive to consider the statistical shift in this context. Both the Fermi energy E_F and the interface potential V_0 depend on temperature. For the moment we assume that this temperature dependence is linear, i.e.,

$$E_V - E_F = E_V - E_F^0 + \alpha T \tag{32}$$

and

$$eV_0 = eV_0^0 + (\alpha - \beta)T. \tag{33}$$

α and β are constants and E_F^0 and V_0^0 are the Fermi energy and the interface potential at $T=0$ K. From Eqs. (32) and (33) we see that $E_V - E_F - eV_0 = E_V - E_F^0 - eV_0^0 + \beta T$. If this is introduced into Eq. (29) we have, within this linear approximation, a constant prefactor $\exp(\beta/k)$ and the activation energy E_a'' is in fact a better approximation of the difference between the Fermi energy and the valence-band edge at the insulator-semiconductor interface at $T=0$ K, i.e.,

$$E_a'' \approx E_V - E_F^0 - eV_0^0. \tag{34}$$

Nevertheless, the energy scale is not corrected for the statistical shift for the present method. The trap DOS is simply plotted as a function of E_a''. Neglecting the statistical shift is a common feature of all analytical methods in the present comparison that employ temperature-dependent measurements (all methods except for the method by Grünewald *et al.*).

Again, we assumed that $E_V - E_F = 0.5$ eV and $V_{FB} = -4.6$ V. In order to determine the activation energy E_a'' with Eq. (30), the field-effect mobilities were calculated with Eq. (13) leading to a mobility that increases monotonically with gate voltage at all temperatures. These functions were evaluated at $V_g = -50$ V. The mobilities at 299, 289, 280, 270, 259, and 249 K, respectively, are $\mu = 0.17$, 0.16, 0.15, 0.13, 0.11, and 0.09 $\mathrm{cm}^2/\mathrm{Vs}$.[58] E_a'' is significantly different from the activation energy E_a (Fig. 5). Again, the activation energy E_a'' was represented by a smooth fit in order to suppress the noise in the data (red line in Fig. 5). The smoothed function was used for the calculation of the trap DOS.

4. Method by Grünewald et al.

This method does not require temperature-dependent measurements.[8,10,13,59] It allows to convert a single transfer characteristic into the underlying density-of-states function which may be advantageous in certain situations where temperature-dependent measurements are not possible.[59] In addition, it is not necessary to consider the temperature dependence of the Fermi energy, the interface potential, or the band mobility. Moreover, the method is not based on the abrupt approximation. The interface potential V_0 as a function of gate voltage is calculated from

$$\exp\left(\frac{eV_0}{kT}\right) - \frac{eV_0}{kT} - 1 = \frac{e}{kT}\frac{\epsilon_i d}{\epsilon_s l \sigma_0}\left[U_g \sigma(U_g) - \int_0^{U_g} \sigma(\tilde{U}_g) d\tilde{U}_g\right]. \tag{35}$$

For each gate voltage, Eq. (35) is numerically evaluated using the measured field-effect conductivity σ [Eq. (12)]. Eventually, we have the complete function $V_0 = V_0(V_g)$. The total hole density p can be calculated with V_0 according to

$$p(V_0) = \frac{\epsilon_0 \epsilon_i^2}{\epsilon_s l^2 e} U_g \left(\frac{dV_0}{dU_g}\right)^{-1}. \tag{36}$$

Within the zero-temperature approximation the trap DOS $N(E)$ can then be written as

$$N(E) \approx \frac{1}{e}\frac{dp(V_0)}{dV_0}. \tag{37}$$

This means that we do a numerical differentiation of the hole density from Eq. (36) with respect to the interface potential V_0 from Eq. (35). The trap DOS can be plotted as a function of the energy $E = eV_0$, i.e., as a function of the energy relative to the Fermi energy E_F. It can also be plotted as a function of the energy $E = E_V - E_F - eV_0$ which requires the difference $E_V - E_F$ to be estimated.

For the present method, the gated four-terminal measurement at $T = 299$ K was considered. Again, we assumed $E_V - E_F = 0.5$ eV and $V_{FB} = -4.6$ V.

5. Method I by Kalb et al.

The free hole density P_{free} per unit area is written as

$$P_{free} \approx a(V_g) N_V \exp\left(-\frac{E_V - E_F - eV_0}{kT}\right) \tag{38}$$

with

$$a(V_g) = \frac{m}{2m-1}\frac{2kT\epsilon_0\epsilon_s}{eC_i U_g}. \tag{39}$$

$a(V_g)$ is the effective thickness of the accumulation layer. $E_0 = kT_0$ is the slope of the trap DOS and $m = T_0/T$.[32] Since the field-effect conductivity can be written as

$$\sigma = e\mu_0 P_{free} \tag{40}$$

the difference $E_V - E_F - eV_0$ is approximated by the activation energy $E_a(V_g)$ of the field-effect conductivity σ. E_a is determined with linear regressions from the measured data according to Eq. (15). This procedure implies that the temperature dependence of the mobility μ_0 as well as the temperature dependence of the effective accumulation-layer thickness a is negligible compared to the exponential temperature dependence. By substituting $dV_0 = -dE_a/e$ in Eqs. (36) and (37), we finally have the trap DOS

$$N(E) \approx \frac{d}{dE_a}\left[\frac{\epsilon_0 \epsilon_i^2}{\epsilon_s l^2} U_g \left(\frac{dE_a}{dU_g}\right)^{-1}\right] \tag{41}$$

as a function of the energy $E = E_a(V_g) \approx E_V - E_F - eV_0$.

The band mobility μ_0 can be estimated with

$$\mu_0 = \sigma/(eP_{free}), \tag{42}$$

where σ is the measured field-effect conductivity and P_{free} is calculated according to Eq. (38).[32] Importantly, the parameters E_0 and m are not relevant for the calculation of the trap DOS with Eq. (41). Equations (38) and (39) only explain the use of the activation energy in Eq. (41).

We give some specific details about the use of this method: we used $V_{FB}=-4.6$ V. The trap DOS was calculated with Eq. (41) from the smooth fit of the activation energy E_a in Fig. 5. The parameter $m=T_0/T$ in Eq. (39) is only relevant for the calculation of the band mobility μ_0 with Eq. (42). To obtain this parameter, an exponential function $N(E)=N_0 \exp(-E/E_0)$ was fitted to the trap DOS that had previously been obtained with Eq. (41). This gave $E_0=kT_0=60$ meV and thus $m=2.33$ at $T=299$ K. The band mobility was calculated for a gate voltage of $V_g=-50$ V and $T=299$ K.

6. Method II by Kalb et al.

As suggested by Fortunato *et al.*, the temperature dependence of the band mobility μ_0 can be eliminated by calculating a normalized field-effect conductivity σ' for each temperature according to Eq. (28). In order to improve upon the method by Kalb *et al.*, the normalized activation energy $E_a'(V_g)$ is determined for each gate voltage with a linear regression according to

$$\sigma'(V_g) \propto \exp\left(-\frac{E_a'}{kT}\right). \tag{43}$$

σ' in Eq. (43) is the normalized field-effect conductivity according to Eq. (28). E_a' is a better approximation of the difference between the Fermi energy and the valence-band edge, i.e., we now have

$$E_a' \approx E_V - E_F - eV_0. \tag{44}$$

E_a' is now used instead of E_a in Eq. (41), i.e., the trap DOS is finally calculated with

$$N(E) \approx \frac{d}{dE_a'}\left[\frac{\epsilon_0\epsilon_i^2}{\epsilon_s l^2} U_g \left(\frac{dE_a'}{dU_g}\right)^{-1}\right]. \tag{45}$$

It is plotted as a function of the energy $E=E_a' \approx E_V - E_F - eV_0$.

7. Influence of the choice of parameters

We also investigated how the choice of the effective accumulation-layer thickness a and the difference between the Fermi level and the valence-band edge far from the insulator-semiconductor interface E_V-E_F effect the final result. The effective accumulation-layer thickness a needs to be fixed for the method by Lang *et al.* Clearly, this choice significantly affects the trap DOS (Fig. 7). For the method by Horowitz *et al.*, $E_V-E_F=0.5$ eV was chosen. We repeated the calculations for $E_V-E_F=0.8$ eV and again, the trap densities from the measurements at different temperatures were found to coincide with a parameter of $\mu_0=0.2$ cm^2/Vs. The results are compared in Fig. 7. The slope of the trap DOS calculated for $E_V-E_F=0.5$ and 0.8 eV are almost identical in both cases but the trap densities are reduced to some extend due to the larger value of eV_0 in the denominator of Eq. (22). Also for the method by Fortunato *et al.*, the parameter E_V-E_F needs to be known. However, this method is not sensitive to the choice of this parameter: calculations for $E_V-E_F=0.8$ eV give essentially the same result. Clearly, for the method by Günewald *et al.*, the guess of E_V-E_F has a significant influence on the trap DOS since the energy scale is given by $E_V-E_F-eV_0$ and only eV_0 is known. Therefore, the choice of $E_V-E_F=0.8$ eV instead of 0.5 eV leads to a parallel shift of the trap DOS by 0.3 eV along the energy scale as shown in Fig. 7. For the methods by Kalb *et al.* (method I and II) we neither need to make an assumptions about E_V-E_F nor about the effective accumulation-layer thickness a.

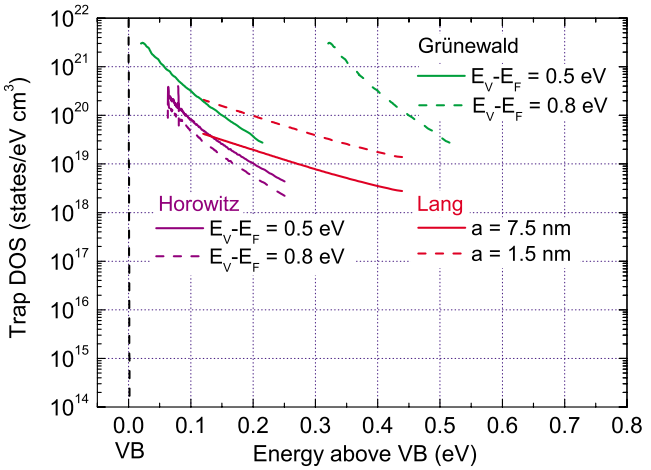

FIG. 7. (Color online) The choice of certain parameters in the analytical methods can have a significant effect on the trap DOS. For the method by Lang *et al.*, an effective accumulation layer thickness of $a=1.5$ nm (dashed red line) instead of 7.5 nm (full red line) leaves the slope of the trap DOS unchanged but leads to a significant increase in the overall trap densities. For the method by Horowitz *et al.*, the use of $E_V-E_F=0.8$ eV (dashed violet line) instead of $E_V-E_F=0.5$ eV (full violet line) results in a rather small change in the magnitude of the trap densities. The method by Grünewald *et al.* very sensitively depends on the choice of E_V-E_F: using $E_V-E_F=0.8$ eV (dashed green line) instead of $E_V-E_F=0.5$ eV (full green line) results in a parallel shift of the trap DOS by 0.3 eV.

The necessity to choose the effective density of extended states ($N_V=3\times10^{21}$ cm^{-3} in the present study) leads to an uncertainty in the absolute value of the band mobility. The volume density of extended states is given by the density of the pentacene molecules ($\approx3\times10^{21}$ cm^{-3}) multiplied by two due to the spin degree of freedom.[42,60,61] However, a value of $\approx6\times10^{21}$ cm^{-3} is likely to overestimate the effective density of extended states N_V. The underlying spectral density of extended states (in cm^{-3} eV^{-1}) should drop close to the valence-band edge. The extended states close to the valence-band edge are the most important contribution to N_V though. Therefore, the volume density of molecules without the degeneracy factor (Ref. 32) or even half the molecular density (Ref. 21) have been used as approximations of N_V. In

the case of pentacene, a value as low as $N_V=1\times10^{21}$ cm^{-3} has also been used.[41] From the method by Horowitz *et al.* it appears, that N_V cannot be higher than 3×10^{21} cm^{-3}. A band mobility of $\mu_0=0.2$ cm^2/Vs was calculated from the product $\mu_0 N_V$ with $N_V=3\times10^{21}$ cm^{-3}: a larger N_V would lead to a band mobility lower than the field-effect mobility which would not be a reasonable result.[58]

B. Computer simulation of the transfer characteristics

For the modeling of the transfer characteristics, we used the Matlab®-based program developed by Oberhoff *et al.*[40] The essence of this approach is that the program calculates the transfer characteristics from the trap DOS, the spectral density of extended states and the band mobility μ_0. It is assumed that the valence band has a rectangular shape, i.e., the density of extended states (in cm^{-3} eV^{-1}) is constant anywhere in the valence band.[40] The program can simulate the transfer characteristic at any temperature T as long as the band mobility μ_0 at this temperature is also fixed *a priori*. The full Fermi-Dirac statistics is included.[40] This means that, in contrast to the analytical methods, the Fermi function is not approximated and the temperature dependence of the Fermi energy E_F is not neglected. In Fig. 3 we show simulated transfer characteristics (red lines) closely matching the measured data (symbols). The trap DOS from which these transfer characteristics were calculated is also shown in Fig. 4 (light blue line). Table I lists the respective parameters including the band mobility at RT.

We now give some more specific details about the simulations. The program allows for a consideration of parasitic resistances at the source and drain contacts. For the present simulations, we have however assumed negligible contact resistances. This is supported by the gated four-terminal measurements, which show that the total contact resistance is significantly lower than the channel resistance at all temperatures. More specifically at $V_g=-50$ V and $T=299$ K, the channel resistance is about ten times larger than the contact resistance and still five times larger than the contact resistance at $V_g=-50$ V and $T=249$ K. We use 10^{22} cm^{-3} eV^{-1} for the density of extended states in the rectangular band. In essence, this is an approximation of the density of extended states close to the valence-band edge since only these states are of importance for the charge transport. The value is lower by a factor of 2 compared to the volume density of extended states (6×10^{21} cm^{-3}) divided by the bandwidth (0.3 eV, Ref. 62). The reduced value accounts for a drop of the spectral density of extended states close to the valence-band edge in analogy to the choice of $N_V=3\times10^{21}$ cm^{-3} for the analytical methods. To obtain a good fit of the transfer characteristics at all temperatures, it was necessary to allow for a temperature dependence of the band mobility μ_0. For the fit in Fig. 3, the band mobilities μ_0 at 299, 289, 280, 270, 259, and 249 K were fixed at 0.32, 0.28, 0.25, 0.21, 0.17, and 0.14 cm^2/Vs, respectively.

IV. DISCUSSION

We begin with a discussion of the results in Fig. 4 and Table I. The estimate from the subthreshold swing assumes the trap densities not to depend on energy. It is derived from the subthreshold swing and can thus be regarded as a rough estimate of the density of traps slightly above the Fermi energy E_F. It is however gratifying to note the agreement between the trap DOS derived from the subthreshold swing (valid for $E\approx E_F$) and the lowest values of the trap DOS from the other methods. All other methods result in a trap DOS that increases somewhat faster than exponentially with energy. From Fig. 4 and Table I we see that the choice of the method to calculate the trap DOS has a considerable effect on the final result.

The method by Kalb *et al.* (method I) gives a good estimate of the slope of the trap DOS but leads to an overestimation of the overall magnitude of the trap densities, i.e., the parameter N_0. This is because the temperature dependence of the band mobility μ_0 in Eq. (40) is neglected compared to the exponential temperature dependence [Eq. (38)]. The improved method by Kalb *et al.* (method II) uses the activation energy E_a' instead of E_a, and E_a' is calculated from the normalized field-effect conductivity at each temperature [Eq. (43)]. This means that the temperature dependence of the band mobility is properly taken account of. The correction has a considerable effect on the overall magnitude of the trap densities. The improved method leads to a trap DOS that is in much better agreement with the other methods and, in particular, with the result from the simulations. This means that the temperature dependence of the band mobility μ_0 should generally not be neglected when calculating the trap DOS with an analytical method. Method II by Kalb *et al.* is similar to the method by Fortunato *et al.* It is easier to be used but is based on additional simplifications. The difference between the method by Fortunato *et al.* and the method II by Kalb *et al.* is the use of the activation energy E_a'' of the derivative $d\sigma'/dV_g$ instead of the activation energy E_a' of σ'. Moreover, V_0 in Eq. (26) is not neglected by Fortunato *et al.*, contrary to the method by Kalb *et al.* Neglecting V_0 does not lead to significant differences for sufficiently high gate voltages since the interface potential is typically less than 0.5 V. On the other hand, from Fig. 5 we see that there are significant differences between E_a' and E_a''. The difference between the two methods, therefore, is almost exclusively due to the use of E_a'' instead of E_a'. The method II by Kalb *et al.* corrects for the temperature dependence of the band mobility but neglects the temperature dependence of $a(V_g)$ [Eq. (39)] against the exponential temperature dependence in Eq. (38). This still is a source of error. For the present example we have $mkT/(2m-1)=16.41$ meV at $T=299$ K, and $mkT/(2m-1)=13.07$ meV at $T=249$ K, i.e., a ratio of 1.26. This should be compared to $\mu^{\mathrm{RT}}/\mu^T=1.9$ ($\mu^{\mathrm{RT}}=0.17$ cm^2/Vs and $\mu^T=0.09$ cm^2/Vs at $T=249$ K). The method by Fortunato *et al.* is in excellent agreement with the result from the computer simulations.

The method by Lang *et al.* leads to a significant error in the slope of the trap DOS. This is mainly due to the assumption of a gate-voltage-independent effective accumulation-layer thickness a. If we allow for a gate-voltage-dependent effective accumulation-layer thickness in the context of the abrupt approximation, the effective thickness $a(V_g)$ decreases with increasing gate voltage [Eq. (39)]. As a consequence, the assumption of a constant thickness a in the de-

nominator of Eq. (18) leads to an overestimation of the trap density at low gate voltages (at energies far from the valence-band edge) and to an underestimation of the trap density at high gate voltages (at energies close to the valence-band edge).

From Fig. 7 we see that some analytical methods do not lead to an unambiguous result. In principle, the difference $E_V - E_F$ may be approximated with the measured activation energy near the flatband condition. However, this activation energy can often not be measured because the off-current of an organic field-effect transistor is often due to experimental limitations and is not related to the conductivity of the organic semiconductor. If $E_V - E_F$ is not experimentally accessible, we have an uncertainty in the trap densities using the methods by Horowitz *et al.* and Grünewald *et al.* as shown in Fig. 7. Moreover, Fig. 7 shows the significant dependence of the result from the method by Lang *et al.* on the choice of the constant effective accumulation-layer thickness a. The methods by Fortunato *et al.* and the methods by Kalb *et al.* do not lead to these uncertainties.

The analytical methods approximate the Fermi function to a step function for the trapped holes and use Boltzmann's approximation for the free holes. The temperature dependencies of the Fermi energy E_F and the interface potential V_0 are also neglected. These assumptions appear to be less restrictive because the trap distributions from most analytical methods are in good agreement with the result from the simulations which do not involve these assumptions.

Most analytical methods lead to a band mobility μ_0 that is comparable to the value of μ_0 from the simulations. It is important to note that the band mobility μ_0 from most methods is only slightly higher than the field-effect mobility μ at high gate voltages, i.e., $\mu \approx 0.2$ cm^2/Vs at $V_g = -50$ V and $T = 299$ K for this sample. Since $\mu = (P_{free}/P)\mu_0$ this means that even in samples with an increased trap density (TFT's), most of the gate-induced holes are free.

For the method by Fortunato *et al.* and for method II by Kalb *et al.*, the activation energy (E_a'' or E_a') is calculated from the normalized field-effect conductivity at each temperature. The field-effect conductivity is normalized to the field-effect mobilities at high gate voltages μ^{RT}/μ^T. This ratio is an approximation of the ratio of the respective band mobilities $\mu_0^{\mathrm{RT}}/\mu_0^T$. For example, the field-effect mobility at $V_g = -50$ V is $\mu^{\mathrm{RT}} = 0.17$ cm^2/Vs at 299 K and $\mu^T = 0.09$ cm^2/Vs at 249 K. This gives a ratio of $\mu^{\mathrm{RT}}/\mu^T = 1.9$.[63] From the simulations we have a band mobility of $\mu_0^{\mathrm{RT}} = 0.32$ cm^2/Vs at 299 K and $\mu_0^T = 0.14$ cm^2/Vs at 249 K. The ratio of the band mobilities thus is $\mu_0^{\mathrm{RT}}/\mu_0^T = 2.3$. These two ratios are very similar, indeed. This further supports the correction of the field-effect conductivity as suggested by Fortunato *et al.*

We also note that from the simulations we have a band mobility μ_0 that decreases as the sample is cooled down. This may indicate that the trap-free transport process is a hopping transport but may also be limited by a thermally activated process at the grain boundaries.

Finally, we recall that the trap DOS was calculated from transistors with a rather small gate capacitance and we thus have relatively large operating voltages. If transistors with a high gate capacitance are to be used in order to quantify the trap DOS great caution is required. Transistors with a sufficiently high gate capacitance can be operated at gate voltages of only a few volts (e.g., 2–3 V).[64,65] This is comparable to the magnitude of the interface potential V_0 (≤ 0.5 V). However, all methods apart from the method by Fortunato *et al.* assume that the total charge per unit area can be approximated according to $C_i(V_g - V_{FB} - V_0) \approx C_i(V_g - V_{FB})$. Significant errors are to be expected if V_0 is neglected for low-voltage operating transistors. The method by Fortunato *et al.* does not neglect V_0 and could thus be used in this scenario. For a low-voltage operating transistor, the choice of the parameter $E_V - E_F$ for the method by Fortunato *et al.* is however expected to be a source of ambiguity because V_0 can no longer be neglected in the numerator of Eq. (26).

V. SUMMARY AND CONCLUSIONS

Several different methods were used to quantify the spectral density of localized states in a pentacene-based organic thin-film transistor. The trap DOS derived from the simple formula for the subthreshold swing is in rather good agreement with the lowest values of the trap DOS from the other, more sophisticated methods. Most methods result in an almost exponential trap DOS close to the valence-band edge with a typical slope of 50 meV. We find that the choice of the method to calculate the trap DOS has a considerable effect on the final result. More specifically, two assumptions lead to significant errors in the trap DOS. First, neglecting the temperature dependence of the band mobility can lead to a rather large overestimation of the trap densities. Second, the assumption of a gate-voltage-independent effective accumulation-layer thickness results in a significant underestimation of the slope of the trap DOS. A general conclusion of this study is that it is necessary to consider the specific deviations of a given calculation method if one compares energetic distributions of trap states from organic field-effect transistors evaluated by different groups with different methods.

The methods by Fortunato *et al.* and the method II by Kalb *et al.* do not lead to ambiguities due to the choice of parameters, and this constitute a significant advantage. The computer simulations do not approximate the Fermi function and may therefore be seen as the most reliable result. Simulating the transfer characteristics at various temperatures can, however, be a time consuming endeavor due to the large number of possibilities to fix the trap DOS and the band mobilities. While all methods have their advantages and disadvantages, the method by Fortunato *et al.* is relatively easy to use and gives an unambiguous result in excellent agreement with the computer simulations.

ACKNOWLEDGMENTS

The authors thank Simon Haas and Andreas Reinhard for the growth of pentacene crystals and Thomas Mathis and Kurt Pernstich for valuable discussions.

*kalb@phys.ethz.ch

[1] D. Braga and G. Horowitz, Adv. Mater.(Weinheim, Ger.) **21**, 1473 (2009).

[2] H. Sirringhaus, Adv. Mater. **21**, 3859 (2009).

[3] T. W. Kelley, D. V. Muyres, P. F. Baude, T. P. Smith, and T. D. Jones, *Organic and Polymeric Materials and Devices*, MRS Symposia Proceedings No. 771 (Materials Research Society, Pittsburgh, 2003), p. L6.5.1.

[4] X.-H. Zhang, B. Domercq, and B. Kippelen, Appl. Phys. Lett. **91**, 092114 (2007).

[5] J. Takeya, J. Kato, K. Hara, M. Yamagishi, R. Hirahara, K. Yamada, Y. Nakazawa, S. Ikehata, K. Tsukagoshi, Y. Aoyagi, T. Takenobu, and Y. Iwasa, Phys. Rev. Lett. **98**, 196804 (2007).

[6] I. McCulloch, M. Heeney, C. Bailey, K. Genevicius, I. MacDonald, M. Shkunov, D. Sparrowe, S. Tierney, R. Wagner, W. M. Zhang, M. L. Chabinyc, R. J. Kline, M. D. McGehee, and M. F. Toney, Nature Mater. **5**, 328 (2006).

[7] W. E. Spear and P. G. Le Comber, J. Non-Cryst. Solids **8-10**, 727 (1972).

[8] M. Grünewald, P. Thomas, and D. Würtz, Phys. Status Solidi B **100**, K139 (1980).

[9] W. E. Spear, D. Allan, P. Le Comber, and A. Ghaith, Philos. Mag. B **41**, 419 (1980).

[10] M. Grünewald, K. Weber, W. Fuhs, and P. Thomas, J. Phys. (France) **42**, 523 (1981).

[11] R. L. Weisfield and D. A. Anderson, Philos. Mag. B **44**, 83 (1981).

[12] M. J. Powell, Philos. Mag. B **43**, 93 (1981).

[13] K. Weber, M. Grünewald, W. Fuhs, and P. Thomas, Phys. Status Solidi B **110**, 133 (1982).

[14] F. Djamdji and P. G. Le Comber, Philos. Mag. B **56**, 31 (1987).

[15] R. Schumacher, P. Thomas, K. Weber, W. Fuhs, F. Djamdji, P. G. Le Comber, and R. E. I. Schropp, Philos. Mag. B **58**, 389 (1988).

[16] G. Fortunato and P. Migliorato, Appl. Phys. Lett. **49**, 1025 (1986).

[17] P. Migliorato and D. B. Meakin, Appl. Surf. Sci. **30**, 353 (1987).

[18] G. Fortunato, D. B. Meakin, P. Migliorato, and P. G. Le Comber, Philos. Mag. B **57**, 573 (1988).

[19] V. Foglietti, L. Mariucci, and G. Fortunato, J. Appl. Phys. **85**, 616 (1999).

[20] J. Sun, D. A. Mourey, D. Zhao, and T. N. Jackson, J. Electron. Mater. **37**, 755 (2008).

[21] G. Horowitz, R. Hajlaoui, and P. Delannoy, J. Phys. III **5**, 355 (1995).

[22] F. Schauer, J. Appl. Phys. **86**, 524 (1999).

[23] I. Zhivkov, S. Nešpurek, and F. Schauer, Adv. Mater. Opt. Electron. **9**, 175 (1999).

[24] G. Horowitz, M. E. Hajlaoui, and R. Hajlaoui, J. Appl. Phys. **87**, 4456 (2000).

[25] D. V. Lang, X. Chi, T. Siegrist, A. M. Sergent, and A. P. Ramirez, Phys. Rev. Lett. **93**, 086802 (2004).

[26] F. De Angelis, S. Cipolloni, L. Mariucci, and G. Fortunato, Appl. Phys. Lett. **88**, 193508 (2006).

[27] F. De Angelis, L. Mariucci, S. Cipolloni, and G. Fortunato, J. Non-Cryst. Solids **352**, 1765 (2006).

[28] W. L. Kalb, T. Mathis, S. Haas, A. F. Stassen, and B. Batlogg, Appl. Phys. Lett. **90**, 092104 (2007).

[29] N. Kawasaki, T. Nagano, Y. Kubozono, Y. Sako, Y. Morimoto, Y. Takaguchi, A. Fujiwara, C. C. Chu, and T. Imae, Appl. Phys. Lett. **91**, 243515 (2007).

[30] W.-Y. So, J. M. Wikberg, D. V. Lang, O. Mitrofanov, C. L. Kloc, T. Siegrist, A. M. Sergent, and A. P. Ramirez, Solid State Commun. **142**, 483 (2007).

[31] D. Guo, T. Miyadera, S. Ikeda, T. Shimada, and K. Saiki, J. Appl. Phys. **102**, 023706 (2007).

[32] W. L. Kalb, K. Mattenberger, and B. Batlogg, Phys. Rev. B **78**, 035334 (2008).

[33] W.-Y. So, D. V. Lang, V. Y. Butko, X. Chi, J. C. Lashley, and A. P. Ramirez, J. Appl. Phys. **104**, 054512 (2008).

[34] M. Leufgen, O. Rost, C. Gould, G. Schmidt, J. Geurts, L. W. Molenkamp, N. S. Oxtoby, M. Mas-Torrent, N. Crivillers, J. Veciana, and C. Rovira, Org. Electron. **9**, 1101 (2008).

[35] C. Vanoni, T. A. Jung, and S. Tsujino, Appl. Phys. Lett. **94**, 253306 (2009).

[36] A. R. Völkel, R. A. Street, and D. Knipp, Phys. Rev. B **66**, 195336 (2002).

[37] S. Scheinert, G. Paasch, M. Schrödner, H.-K. Roth, S. Sensfuß, and T. Doll, J. Appl. Phys. **92**, 330 (2002).

[38] A. Salleo, T. W. Chen, A. R. Völkel, Y. Wu, P. Liu, B. S. Ong, and R. A. Street, Phys. Rev. B **70**, 115311 (2004).

[39] D. Knipp, P. Kumar, A. R. Völkel, and R. A. Street, Synth. Met. **155**, 485 (2005).

[40] D. Oberhoff, K. P. Pernstich, D. J. Gundlach, and B. Batlogg, IEEE Trans. Electron Devices **54**, 17 (2007).

[41] S. Scheinert, K. P. Pernstich, B. Batlogg, and G. Paasch, J. Appl. Phys. **102**, 104503 (2007).

[42] K. P. Pernstich, B. Rössner, and B. Batlogg, Nature Mater. **7**, 321 (2008).

[43] E. A. Silinsh and V. Čápek, *Organic Molecular Crystals* (AIP, New York, 1994).

[44] V. I. Arkhipov, E. V. Emelianova, and G. J. Adriaenssens, Phys. Rev. B **64**, 125125 (2001).

[45] S. M. Sze, *Physics of Semiconductor Devices* (Wiley, New York, 1981).

[46] A. Rolland, J. Richard, J. P. Kleider, and D. Mencaraglia, J. Electrochem. Soc. **140**, 3679 (1993).

[47] M. McDowell, I. G. Hill, J. E. McDermott, S. L. Bernasek, and J. Schwartz, Appl. Phys. Lett. **88**, 073505 (2006).

[48] M. H. Yoon, C. Kim, A. Facchetti, and T. J. Marks, J. Am. Chem. Soc. **128**, 12851 (2006).

[49] G. Horowitz, R. Hajlaoui, D. Fichou, and A. El Kassmi, J. Appl. Phys. **85**, 3202 (1999).

[50] G. Horowitz, P. Lang, M. Mottaghi, and H. Aubin, Adv. Funct. Mater. **14**, 1069 (2004).

[51] M. Shur and M. Hack, J. Appl. Phys. **55**, 3831 (1984).

[52] M. Matters, D. M. de Leeuw, M. J. C. M. Vissenberg, C. M. Hart, P. T. Herwig, T. Geuns, C. M. J. Mutsaers, and C. J. Drury, Opt. Mater. **12**, 189 (1999).

[53] M. Schubert, C. Bundesmann, G. Jacopic, H. Maresch, and H. Arwin, Appl. Phys. Lett. **84**, 200 (2004).

[54] M. Mottaghi and G. Horowitz, Org. Electron. **7**, 528 (2006).

[55] J. Takeya, C. Goldmann, S. Haas, K. P. Pernstich, B. Ketterer, and B. Batlogg, J. Appl. Phys. **94**, 5800 (2003).

[56] P. V. Pesavento, R. J. Chesterfield, C. R. Newman, and C. D. Frisbie, J. Appl. Phys. **96**, 7312 (2004).

[57] V. Y. Butko, X. Chi, D. V. Lang, and A. P. Ramirez, Appl. Phys. Lett. **83**, 4773 (2003).

[58] Alternatively, Eq. (14) could be used to calculate the field-effect mobility. Equation (14) also leads to mobilities that increase

monotonically with gate voltage at all temperatures. The absolute values of the mobilities are lower, however. At $V_g=-50$ V and with $V_{FB}=-4.6$ V we have mobilities of 0.082, 0.071, 0.062, 0.051, 0.041, and 0.032 cm^2/Vs ($T=299$, 289, 280, 270, 259, and 249 K).

[59] W. L. Kalb, F. Meier, K. Mattenberger, and B. Batlogg, Phys. Rev. B **76**, 184112 (2007).

[60] S. Scheinert and G. Paasch, Phys. Status Solidi A **201**, 1263 (2004).

[61] K. P. Pernstich, D. Oberhoff, C. Goldmann, and B. Batlogg, Appl. Phys. Lett. **89**, 213509 (2006).

[62] D. Nabok, P. Puschnig, C. Ambrosch-Draxl, O. Werzer, R. Resel, and D.-M. Smilgies, Phys. Rev. B **76**, 235322 (2007).

[63] If the mobilities are calculated with Eq. (14), we get a ratio of $\mu^{RT}/\mu^T=2.6$.

[64] H. Klauk, U. Zschieschang, R. T. Weitz, H. Meng, F. Sun, G. Nunes, D. E. Keys, C. R. Fincher, and Z. Xiang, Adv. Mater. (Weinheim, Ger.) **19**, 3882 (2007).

[65] M. P. Walser, W. L. Kalb, T. Mathis, and B. Batlogg, Appl. Phys. Lett. **95**, 233301 (2009).